

# Interaction of the Noncovalent Molecular Adapter, $\beta$ -Cyclodextrin, with the Staphylococcal $\alpha$ -Hemolysin Pore

Li-Qun Gu\* and Hagan Bayley\*<sup>†</sup>

\*Department of Medical Biochemistry and Genetics, The Texas A & M University System Health Science Center, College Station, Texas 77843-1114, and <sup>†</sup>Department of Chemistry, Texas A & M University, College Station, Texas 77843-3255 USA

**ABSTRACT** Cyclodextrins act as noncovalent molecular adapters when lodged in the lumen of the  $\alpha$ -hemolysin ( $\alpha$ HL) pore. The adapters act as binding sites for channel blockers, thereby offering a basis for the detection of a variety of organic molecules with  $\alpha$ HL as a biosensor element. To further such studies, it is important to find conditions under which the dwell time of cyclodextrins in the lumen of the pore is extended. Here, we use single-channel recording to explore the pH- and voltage-dependence of the interaction of  $\beta$ -cyclodextrin ( $\beta$ CD) with  $\alpha$ HL.  $\beta$ CD can access its binding site only from the *trans* entrance of pores inserted from the *cis* side of a bilayer. Analysis of the binding kinetics shows that there is a single binding site for  $\beta$ CD, with an apparent equilibrium dissociation constant that varies by >100-fold under the conditions explored. The dissociation rate constant for the neutral  $\beta$ CD molecule varies with pH and voltage, a result that is incompatible with two states of the  $\alpha$ HL pore, one of high and the other of low affinity. Rather, the data suggest that the actual equilibrium dissociation constant for the  $\alpha$ HL  $\cdot$   $\beta$ CD complex varies continuously with the transmembrane potential.

## INTRODUCTION

The engineering of ion channels and pores in order to mimic and improve upon the structures found in nature could have applications in many areas of biotechnology (Bayley, 1997, 1999), including cell permeabilization for cryopreservation (Eroglu et al., 2000), the development of cytotoxic agents (Pederzoli et al., 1995; Al-yahyaee and Ellar, 1996; Panchal et al., 1996), and the construction of biosensors (Ziegler and Göpel, 1998; Bayley, 1999; Bayley et al., 2000).  $\alpha$ -Hemolysin ( $\alpha$ HL), an exotoxin secreted by the bacterium *Staphylococcus aureus* (Gouaux, 1998), is a particularly attractive target for protein engineering. The  $\alpha$ HL pore is a heptamer made of identical subunits of 293 amino acids. Roughly globular molecules with molecular masses of up to  $\sim$ 2000 Da (Füssle et al., 1981), or larger elongated polymers such as single-stranded nucleic acids (Kasianowicz et al., 1996), can pass through a wide channel centered on the molecular sevenfold axis (Fig. 1 *A*).

Earlier engineering studies focused on manipulating the assembly of the pore from monomers. It proved possible to control assembly with chemical, biochemical, and physical stimuli (e.g., divalent metal ions (Walker et al., 1995), proteases (Panchal et al., 1996), and light (Chang et al., 1995)). More recently, guided by the availability of a crystal structure of the heptamer (Song et al., 1996), greater attention has been given to manipulating the properties of the fully assembled pore. For example, binding sites formed by mutagenesis have been placed in the lumen of heteromeric

pores to yield components for metal ion biosensors (Braha et al., 1997); ionic currents flowing through individual engineered pores are modulated by metal ion analytes, and the signal reveals both the concentration and identity of the ions. Single molecule detection of this kind is termed stochastic sensing (Braha et al., 1997; Bayley et al., 2000). Recently, targeted covalent modification has been used to place polymers in the lumen of the pore, increasing the variety of potential biosensor elements (Howorka et al., 2000).

We have also established a new stochastic sensing system by using  $\alpha$ HL equipped with noncovalent cyclodextrin adapters to mediate the sensing of organic molecules (Gu et al., 1999) (Fig. 1, *A* and *B*). Cyclodextrins are well-known to encapsulate organic molecules in aqueous solution and have been widely used in the food and pharmaceutical industries for this purpose (D'Souza and Lipkowitz, 1998).  $\beta$ -Cyclodextrin ( $\beta$ CD) is a cyclic molecule with a hydrophobic cavity, comprising seven D-glucose units. The primary 6-hydroxyl groups are on the narrower rim of the molecule, and the secondary 2- and 3-hydroxyl groups on the wider rim (Fig. 1 *B*). When  $\beta$ CD or other cyclodextrins are lodged in the lumen of the  $\alpha$ HL pore, they alter the unitary conductance (Gu et al., 1999), change the ionic selectivity (Gu et al., 2000), and act as binding sites for channel blockers by contributing their host properties (Gu et al., 1999). The blocker sites provide for the detection of a wide variety of organic molecules.

Further studies of the interactions of cyclodextrins with the  $\alpha$ HL pore will advance the engineering of ion channels and aid the construction of biosensors. In particular, it is important to maximize the dwell time of cyclodextrins within the lumen of the pore. Here, we describe the sidedness, voltage-dependence, and pH-dependence of the interaction of  $\beta$ CD with the wild-type  $\alpha$ HL pore.  $\beta$ CD binds from the *trans* side of the lipid bilayer, with an apparent

Received for publication 14 April 2000 and in final form 7 July 2000.

Address reprint requests to Hagan Bayley, Ph.D., Dept. of Medical Biochemistry and Genetics, The Texas A & M University System Health Science Center, 440 Reynolds Medical Building, College Station, TX 77843-1114. Tel.: 409-845-7047; Fax: 409-862-2416; E-mail: bayley@tamu.edu.

© 2000 by the Biophysical Society

0006-3495/00/10/1967/09 \$2.00

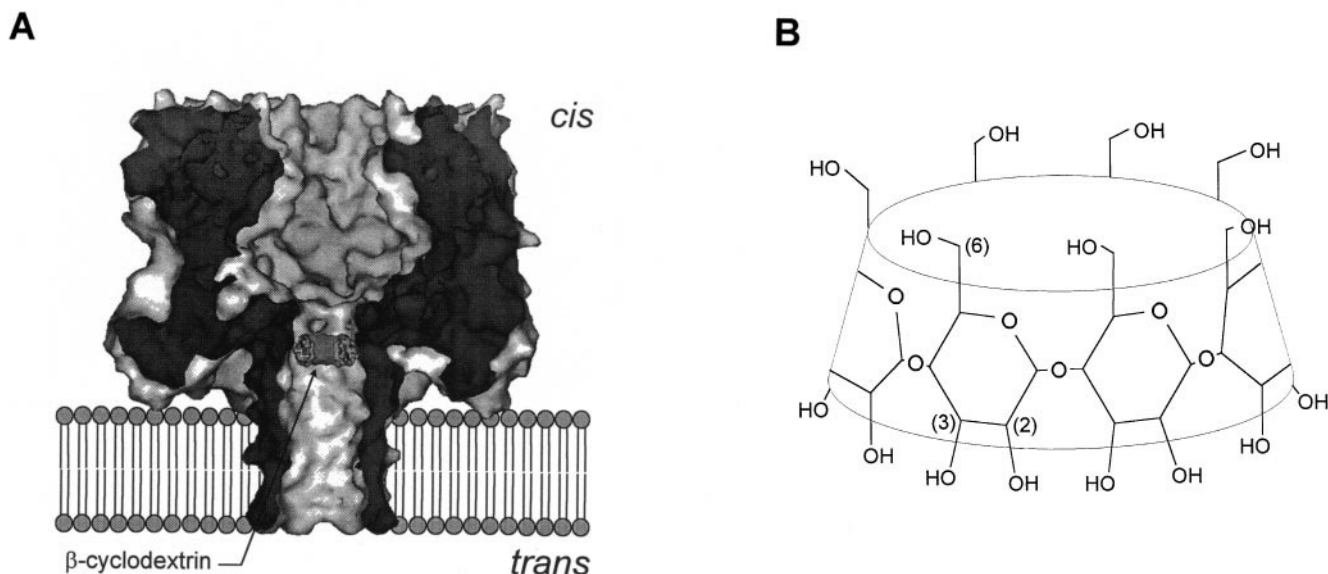


FIGURE 1 Representations of  $\alpha$ -hemolysin ( $\alpha$ HL) and  $\beta$ -cyclodextrin ( $\beta$ CD). (A) Sagittal section through the WT- $\alpha$ HL pore showing  $\beta$ CD lodged in the lumen of the channel. The location is based on mutagenesis data (Gu et al., 1999); (B) structure of  $\beta$ CD.

dissociation constant ( $K_d^{\text{app}}$ ) that varies over a range of  $>100$ -fold.

## MATERIALS AND METHODS

### Reagents

$\beta$ -Cyclodextrin ( $\beta$ CD) was from Aldrich (Milwaukee, WI). Buffers for planar bilayer recording contained 1 M NaCl, 10 mM sodium phosphate, and 2 mM citric acid (Sigma, St. Louis, MO) in deionized water (Millipore Corp., Bedford, MA), and were titrated to pH 5.0 or 7.5 with 1 M HCl (EMScience, Gibbstown, NJ), and to pH 9.0 and pH 11.0 with 2 M NaOH (EMScience).

### Protein

Heptameric WT- $\alpha$ HL was formed by treating monomeric  $\alpha$ HL, purified from *Staphylococcus aureus*, with deoxycholate (Bhakdi et al., 1981; Walker et al., 1992) and isolated from SDS-polyacrylamide gels as described (Braha et al., 1997).

### Bilayer recordings

A 25- $\mu\text{m}$ -thick Teflon film (Goodfellow, Malvern, MA) with a 100–150- $\mu\text{m}$  diameter orifice was used as a partition between the two chambers (2 ml each) of a Teflon bilayer apparatus. The orifice was pretreated with 1:10 hexadecane (Aldrich)/pentane (HPLC-grade, Burdick and Jackson, Muskegon, MI). A solvent-free planar lipid bilayer membrane of 1,2-diphytanoyl-*sn*-glycero-phosphocholine (Avanti Polar Lipids, Inc., Alabaster, AL) was formed across the orifice (Montal and Mueller, 1972; Hanke and Schlue, 1993). The transmembrane potential was applied with Ag/AgCl electrodes with 1.5% agarose bridges (Ultra Pure DNA Grade, Bio-Rad Laboratories, Hercules, CA) containing 3 M KCl (Sigma). Protein was added to the *cis* chamber, which was at ground. A positive potential indicates a higher potential in the *trans* chamber, and a positive current is

one in which cations flow from the *trans* to the *cis* side. Experiments were conducted at  $22 \pm 2^\circ\text{C}$ .

Single-channel current recordings were obtained by using an Axopatch 200B patch-clamp amplifier (Axon Instruments, Inc., Foster City, CA), in the whole-cell ( $\beta = 1$ ) mode, with a CV-203BU headstage, and filtered at 5 kHz with a built-in low-pass Bessel filter. The data were acquired by computer at a sampling rate of 20 kHz by using a Digidata 1200 A/D converter (Axon) and Clampex 7.0 software (Axon). The data were analyzed with the software pClamp 6.03 (Axon) and Origin (Microcal Software Inc., Northampton, MA). Conductance values were determined by fitting the peaks in amplitude histograms to Gaussian functions. The mean dwell time  $\tau$  at each conductance level was measured by fitting the dwell time distribution to an exponential function.

Experiments were initiated by the addition of heptameric  $\alpha$ HL to the *cis* compartment of the bilayer apparatus to a final concentration of 3–30 ng  $\text{ml}^{-1}$ , with stirring until a single channel inserted into the membrane.  $\beta$ CD was added to the *trans* chamber at 40  $\mu\text{M}$  unless otherwise specified. For the determination of each set of kinetic constants, three or more separate experiments were performed and data acquired for at least 2 min were analyzed. Values for unitary conductance,  $k_{\text{on}}^{\text{app}}$ ,  $k_{\text{off}}$ , and  $K_d^{\text{app}}$  are quoted as the mean  $\pm$  SD.

## RESULTS

### Sidedness of current block by $\beta$ CD

As previously documented (Menestrina, 1986; Bezrukov and Kasianowicz, 1993; Korchev et al., 1995), except at extremes of pH and transmembrane potential, WT- $\alpha$ HL pores exhibited uniform single-channel conductance states of long duration at both negative and positive transmembrane potentials (Table 1 and Fig. 2A, left,  $651 \pm 4$  pS,  $-40$  mV, pH 7.5, 1 M NaCl; right,  $721 \pm 6$  pS,  $+40$  mV, pH 7.5, 1 M NaCl). The addition of 40  $\mu\text{M}$   $\beta$ CD to the *trans* compartment produced reversible partial blockades of the

**TABLE 1** Conductance values and kinetic parameters for αHL and αHL · βCD at ±40 mV

		$g_{\alpha\text{HL}}$ (pS)	$g_{\alpha\text{HL} \cdot \beta\text{CD}}$ (pS)	$k_{\text{on}}^{\text{app}}$ ( $\text{M}^{-1}\text{s}^{-1}$ )	$k_{\text{off}}$ ( $\text{s}^{-1}$ )	$K_d^{\text{app}}$ (M)
pH5.0	−40 mV	683 ± 3	266 ± 7	$9.0 \pm 0.5 \times 10^4$	$3.2 \pm 0.1 \times 10^2$	$3.1 \pm 0.3 \times 10^{-3}$
	+40 mV	746 ± 12	256 ± 7	$5.0 \pm 0.2 \times 10^4$	$7.0 \pm 0.7 \times 10^2$	$1.4 \pm 0.2 \times 10^{-2}$
pH7.5	−40 mV	651 ± 4	240 ± 3	$4.0 \pm 0.3 \times 10^5$	$1.3 \pm 0.1 \times 10^3$	$3.4 \pm 0.4 \times 10^{-3}$
	+40 mV	721 ± 6	253 ± 4	$2.8 \pm 0.2 \times 10^5$	$2.1 \pm 0.2 \times 10^3$	$7.8 \pm 0.3 \times 10^{-3}$
pH9.0	−40 mV	613 ± 2	228 ± 4	$3.3 \pm 0.2 \times 10^5$	$1.7 \pm 0.1 \times 10^3$	$5.2 \pm 0.4 \times 10^{-3}$
	+40 mV	686 ± 6	232 ± 3	$3.1 \pm 0.1 \times 10^5$	$1.9 \pm 0.3 \times 10^3$	$6.0 \pm 0.4 \times 10^{-3}$
pH11	−40 mV	606 ± 7	212 ± 15	$1.3 \pm 0.1 \times 10^5$	$2.7 \pm 0.2 \times 10^3$	$2.1 \pm 0.3 \times 10^{-2}$
	+40 mV	654 ± 3	196 ± 2	$4.4 \pm 0.2 \times 10^5$	$1.2 \pm 0.1 \times 10^3$	$2.6 \pm 0.2 \times 10^{-3}$

Values at other voltages can be found in Fig. 5. Values for unitary conductance ( $g$ ),  $k_{\text{on}}^{\text{app}}$ ,  $k_{\text{off}}$ , and  $K_d^{\text{app}}$  are quoted as the mean ± SD from three or more separate experiments. Calculations were performed at three significant figures and rounded to two significant figures for the kinetic constants.

ionic current (see below). By contrast, no current block was detected when 40 or 80 μM βCD was added from the *cis* side (Fig. 2 *B*), even at the highest voltages (±120 mV) and lowest pH values (pH = 3.0) tested (data not shown).

### pH- and voltage-dependence of the extent of current block by βCD

The reversible partial blockades of the single-channel currents, obtained by the addition of 40 μM βCD to the *trans*

side of a bilayer, were examined further. At pH 5.0 and −40 mV, the conductance was reduced from 683 ± 3 pS (αHL) to 266 ± 7 pS, while βCD was bound (αHL · βCD) (Table 1 and Fig. 2 *C*, *left*). At pH 5.0 and +40 mV, the conductance was reduced from 746 ± 12 pS (αHL) to 256 ± 7 pS (αHL · βCD) (Fig. 2 *C*, *right*). At pH 7.5, blockades of similar amplitude were observed: at −40 mV, from 651 ± 4 pS (αHL) to 240 ± 3 pS (αHL · βCD) (Fig. 2 *D*, *left*), and at +40 mV, from 721 ± 6 pS (αHL) to 253 ± 4 pS (αHL · βCD) (Fig. 2 *D*, *right*). Again, at pH 11, the extent of block

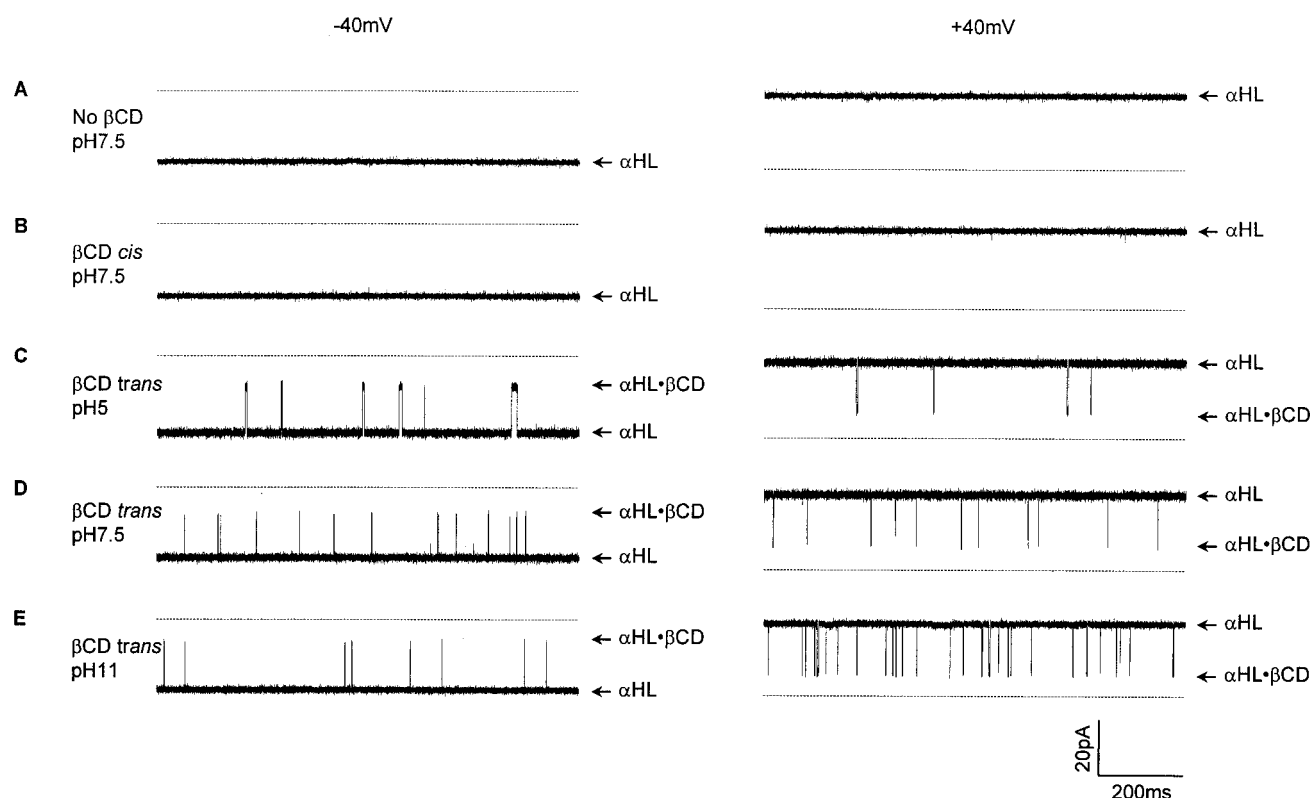


**FIGURE 2** Representative current traces from single αHL pores showing blockades by βCD. All traces were recorded under symmetrical pH conditions in buffer containing 1 M NaCl; 40 μM βCD was added where indicated. *Left*, traces recorded at −40 mV; *right*, traces recorded at +40 mV. The broken line indicates zero current. (A) αHL alone, pH 7.5; (B) αHL with βCD, *cis*, pH 7.5; (C) βCD, *trans*, pH 5.0; (D) βCD, *trans*, pH 7.5; (E) βCD, *trans*, pH 11.0.

was similar: at  $-40$  mV, from  $606 \pm 7$  pS ( $\alpha$ HL) to  $212 \pm 15$  pS ( $\alpha$ HL  $\cdot$   $\beta$ CD) (Fig. 2 E, left), and at  $+40$  mV, from  $654 \pm 3$  pS ( $\alpha$ HL) to  $196 \pm 2$  pS ( $\alpha$ HL  $\cdot$   $\beta$ CD) (Fig. 2 E, right).

A typical amplitude histogram (Fig. 3, inset; recorded at  $-40$  mV, pH 7.5, 1 M NaCl) shows only one current blockade level, which suggests that there is only one binding site for  $\beta$ CD within the lumen of the  $\alpha$ HL pore. The kinetics of the interaction with  $\beta$ CD are also in keeping with this interpretation (see below). The  $I$ - $V$  (current versus voltage) curves for  $\alpha$ HL and  $\alpha$ HL  $\cdot$   $\beta$ CD recorded in 1 M NaCl (Fig. 3) show that neither the conductance of  $\alpha$ HL nor that of  $\alpha$ HL  $\cdot$   $\beta$ CD change dramatically over a wide range of pH values throughout the voltage range from  $-140$  mV to  $+140$  mV.

### $\beta$ CD binds to $\alpha$ HL at a single site in a simple bimolecular interaction

Histograms displaying the dwell time for the unoccupied state of  $\alpha$ HL ( $\tau_{\text{on}}$ ) and the dwell time for  $\beta$ CD in the lumen of the pore ( $\tau_{\text{off}}$ ) could be fitted by single-exponential distributions for data obtained at  $-40$  mV, pH 7.5, 1 M

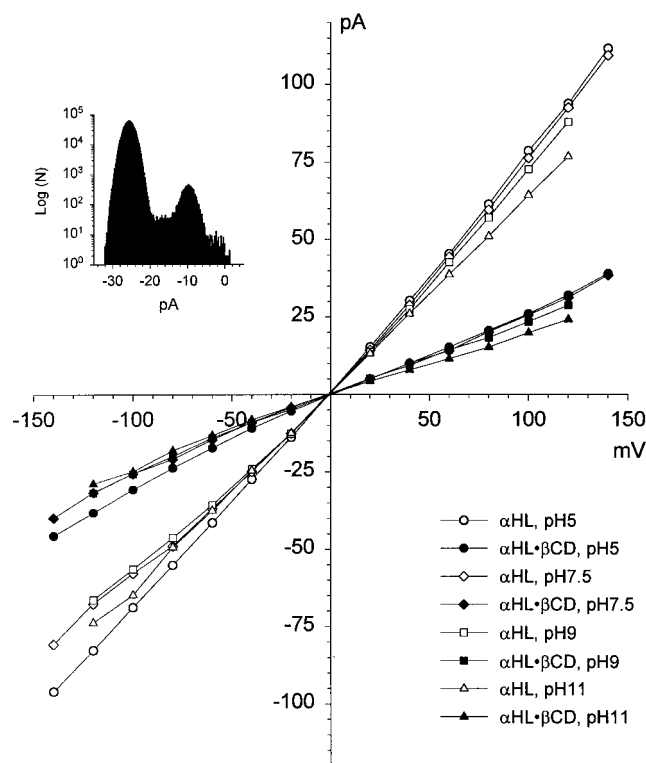
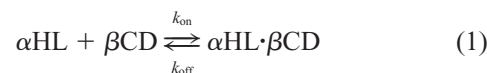


FIGURE 3 Reduction of the unitary conductance of the  $\alpha$ HL pore by  $\beta$ CD. Single-channel  $I$ - $V$  curves for  $\alpha$ HL with or without  $\beta$ CD bound, under different symmetrical pH conditions, as indicated, in 1 M NaCl with  $40 \mu\text{M}$   $\beta$ CD *trans*. Inset, Representative current amplitude histogram from a recording made in the presence of  $40 \mu\text{M}$   $\beta$ CD *trans*, with 1 M NaCl at pH 7.5 in both chambers.

NaCl, and  $40 \mu\text{M}$   $\beta$ CD (Fig. 4, A and B). Single time-constants for both  $\tau_{\text{on}}$  and  $\tau_{\text{off}}$  were also found at the other pH values examined (pH 5.0, pH 9.0 and pH 11.0) and throughout the voltage range  $-140$  to  $+140$  mV (data not shown). These data affirm that, under the wide range of conditions examined here,  $\beta$ CD lodges at a single site in the lumen of the pore, which is accessible from the *trans* side of the bilayer. Therefore, the kinetics of the interaction between  $\beta$ CD and  $\alpha$ HL should obey the simple kinetic scheme:



As expected from Scheme 1, the plot of  $1/\tau_{\text{on}}$  versus  $[\beta\text{CD}]$  was a straight line, the slope of which yields the rate constant  $k_{\text{on}}^{\text{app}}$  (e.g., Fig. 4 C). We use  $k_{\text{on}}^{\text{app}}$  (rather than  $k_{\text{on}}$ ) because certain models for the pH- and voltage-dependence of binding demand more than one state of  $\alpha$ HL. Again, as expected from Scheme 1,  $1/\tau_{\text{off}}$  is independent of  $[\beta\text{CD}]$  (e.g., Fig. 4 D) and  $k_{\text{off}}$  was evaluated as the average of  $1/\tau_{\text{off}}$  at the different  $\beta$ CD concentrations.

### pH- and voltage-dependency of block kinetics

The rate constants,  $k_{\text{on}}^{\text{app}}$  and  $k_{\text{off}}$ , were determined over a wide range of conditions (Fig. 5, A and B). For example, at pH 5.0, at negative transmembrane potentials, the dwell time ( $\tau_{\text{off}}$ ) of  $\beta$ CD in the lumen of the pore (e.g., at  $-40$  mV,  $\tau_{\text{off}} = 3.1 \pm 0.1$  ms,  $k_{\text{off}} = 3.2 \pm 0.1 \times 10^2 \text{ s}^{-1}$ , Fig. 2 C, left) was longer than  $\tau_{\text{off}}$  at positive potentials (e.g., at  $+40$  mV,  $\tau_{\text{off}} = 1.4 \pm 0.2$  ms,  $k_{\text{off}} = 7.0 \pm 0.7 \times 10^2 \text{ s}^{-1}$ , Fig. 2 C, right). By contrast, at pH 5.0,  $\tau_{\text{on}}$  was shorter at negative potentials (at  $-40$  mV and  $40 \mu\text{M}$   $\beta$ CD,  $\tau_{\text{on}} = 280 \pm 20$  ms,  $k_{\text{on}}^{\text{app}} = 9.0 \pm 0.5 \times 10^4 \text{ M}^{-1} \text{ s}^{-1}$ ) than at positive potentials (at  $+40$  mV and  $40 \mu\text{M}$   $\beta$ CD,  $\tau_{\text{on}} = 500 \pm 20$  ms,  $k_{\text{on}}^{\text{app}} = 5.0 \pm 0.2 \times 10^4 \text{ M}^{-1} \text{ s}^{-1}$ ). At pH 11.0, the trends were the opposite of those observed at pH 5.0.  $\tau_{\text{off}}$  was considerably shorter at negative transmembrane potentials (e.g., at  $-40$  mV,  $\tau_{\text{off}} = 0.37 \pm 0.03$  ms,  $k_{\text{off}} = 2.7 \pm 0.2 \times 10^3 \text{ s}^{-1}$ , Fig. 2 E, left) than at positive potentials (e.g., at  $+40$  mV,  $\tau_{\text{off}} = 0.87 \pm 0.04$  ms,  $k_{\text{off}} = 1.2 \pm 0.1 \times 10^3 \text{ s}^{-1}$ , Fig. 2 E, right). At pH 11.0,  $\tau_{\text{on}}$  was longer at negative potentials (at  $-40$  mV and  $40 \mu\text{M}$   $\beta$ CD,  $\tau_{\text{on}} = 190 \pm 10$  ms,  $k_{\text{on}}^{\text{app}} = 1.3 \pm 0.1 \times 10^5 \text{ M}^{-1} \text{ s}^{-1}$ ) than at positive potentials (at  $+40$  mV and  $40 \mu\text{M}$   $\beta$ CD,  $\tau_{\text{on}} = 57 \pm 2$  ms,  $k_{\text{on}}^{\text{app}} = 4.4 \pm 0.2 \times 10^5 \text{ M}^{-1} \text{ s}^{-1}$ ).

Equilibrium dissociation constants ( $K_d^{\text{app}} = k_{\text{off}}/k_{\text{on}}^{\text{app}}$ ) were calculated for  $\alpha$ HL  $\cdot$   $\beta$ CD and differ by over 100-fold under the conditions examined (Fig. 5 C). The most extreme values are seen at pH 5.0 and pH 11.0. For example, at  $-120$  mV,  $\beta$ CD binds 87 times more strongly at pH 5.0 ( $K_d^{\text{app}} = 1.6 \pm 0.1 \times 10^{-3} \text{ M}$ ) than at pH 11.0 ( $K_d^{\text{app}} = 1.4 \pm 0.1 \times 10^{-1} \text{ M}$ ). By contrast, at  $+120$  mV,  $\beta$ CD binds 150 times more strongly at pH 11.0 ( $K_d^{\text{app}} = 7.7 \pm 0.3 \times$



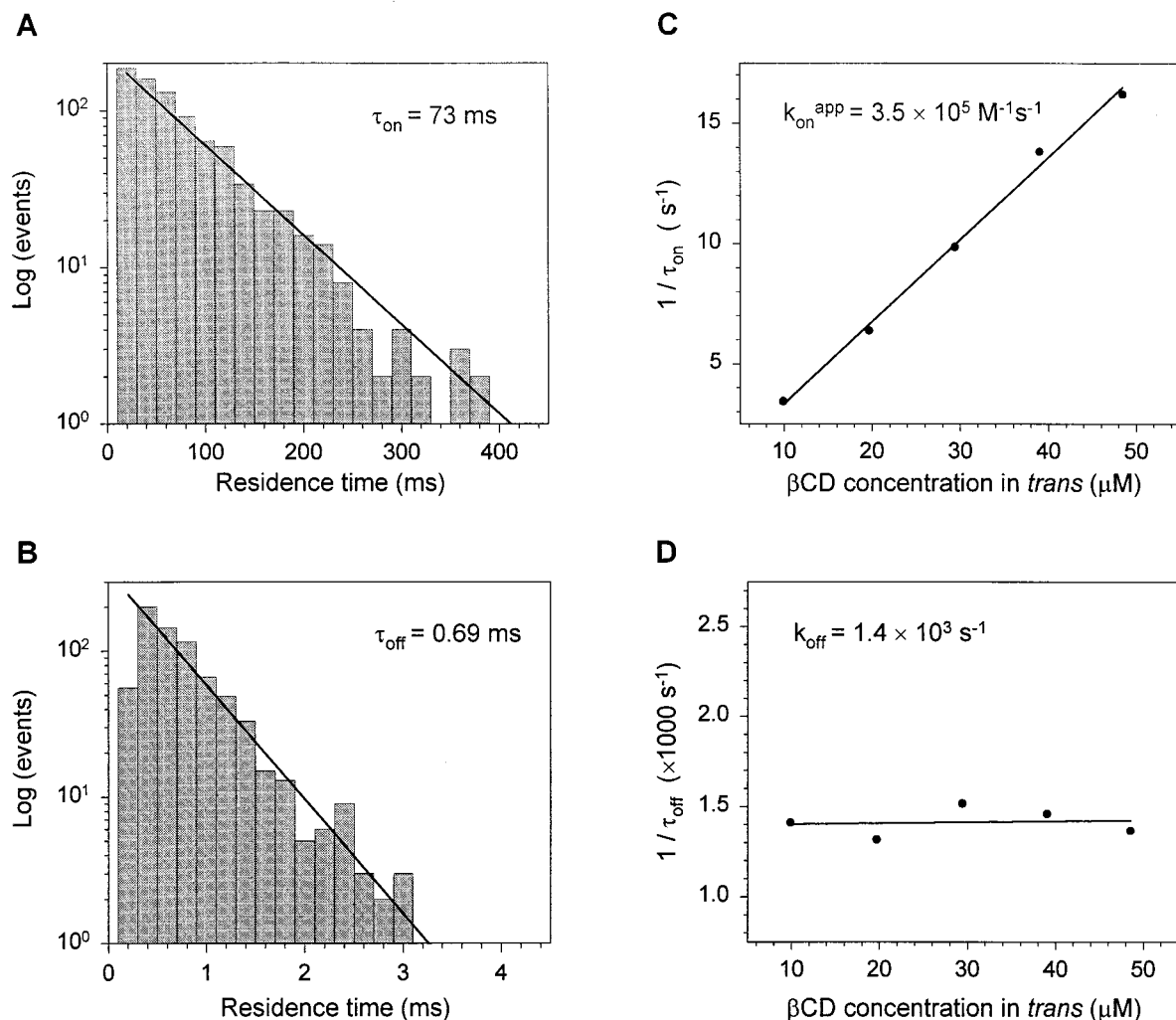


FIGURE 4 Kinetics of the interaction of  $\beta$ CD with  $\alpha$ HL at  $-40$  mV. Dwell time histograms of  $\alpha$ HL (A) and  $\alpha$ HL  $\cdot$   $\beta$ CD (B) were fitted to single-exponential functions. Data were from a recording made with  $40 \mu\text{M}$   $\beta$ CD *trans*, in  $1 \text{ M}$  NaCl at pH 7.5 in both chambers. (C) The rate constant  $k_{\text{on}}^{\text{app}}$  was obtained from the slope of the linear fit of  $1/\tau_{\text{on}}$  versus  $[\beta\text{CD}]$ . (D) The rate constant  $k_{\text{off}}$  is independent of  $[\beta\text{CD}]$  and was obtained from the average of the  $1/\tau_{\text{off}}$  values.

$10^{-4} \text{ M}$ ) than at pH 5.0 ( $K_{\text{d}}^{\text{app}} = 1.1 \pm 0.1 \times 10^{-1} \text{ M}$ ). Interestingly, when extrapolated to a transmembrane potential of  $0 \text{ mV}$ , the  $K_{\text{d}}^{\text{app}}$  values for  $\beta$ CD show little variation over the range pH 5.0 to pH 11.0 (Fig. 5 C). However, it is important to note that changes in both  $k_{\text{on}}^{\text{app}}$  and  $k_{\text{off}}$  occur with pH (Fig. 5, A and B). For example, while the  $K_{\text{d}}^{\text{app}}$  value for  $\beta$ CD at  $0 \text{ mV}$  at pH 5.0 is similar to the  $K_{\text{d}}^{\text{app}}$  value at pH 7.5, compensating changes occur in the on- and off-rate constants.

## DISCUSSION

### $\beta$ CD binds at a specific site within the lumen of the $\alpha$ HL pore

When  $\beta$ CD enters the lumen of the  $\alpha$ HL pore, it reduces the single-channel conductance to 33–43% of the value in the

absence of  $\beta$ CD. The exact value of the reduced conductance varies with the transmembrane potential and the pH of the buffer in the chambers (Fig. 3). Several arguments support the notion that  $\beta$ CD reduces the conductance by binding at a single site within the channel lumen in a defined orientation and conformation.

First, at each pH value and voltage condition, there is only one conductance state that can be assigned to  $\alpha$ HL  $\cdot$   $\beta$ CD (Fig. 3). Second, there is no additional noise associated with the  $\alpha$ HL  $\cdot$   $\beta$ CD state, suggesting that the rather rigid cyclodextrin (Corradini et al., 1996; Schneider et al., 1998; Saenger et al., 1998) is firmly held at the binding site (data not shown, but compare peak widths in Fig. 3 B, *inset*). Third, at all pH values and voltage conditions tested, we find that dwell time histograms for  $\tau_{\text{off}}$  and  $\tau_{\text{on}}$  can be analyzed as single exponentials (Fig. 4, A and B), consistent

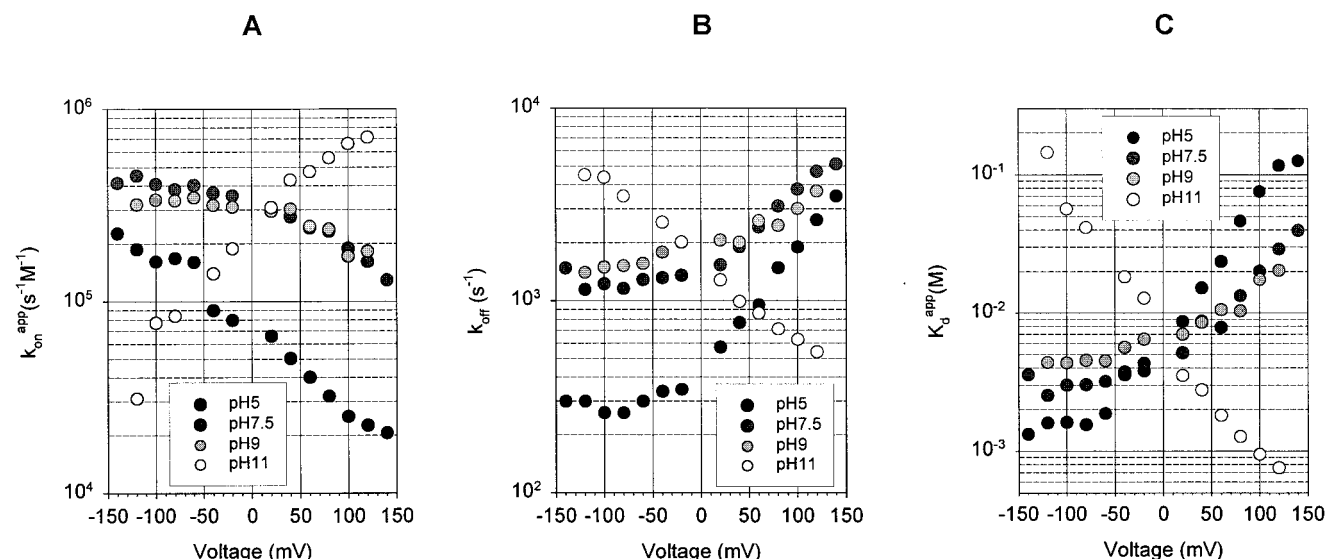


FIGURE 5 Dependence of the kinetic constants for the interaction of  $\beta$ CD with  $\alpha$ HL on pH and voltage. (A)  $k_{on}^{app}$ ; (B)  $k_{off}^{app}$ ; (C)  $K_d^{app}$ . The dissociation constant  $K_d^{app}$  was calculated as  $k_{off}^{app}/k_{on}^{app}$ .

with simple bimolecular kinetics for the interaction of  $\beta$ CD with  $\alpha$ HL (Scheme 1). Fourth, the additional channel block produced when guest molecules bind to  $\beta$ CD lodged in the pore (Gu et al., 1999) suggests that  $\beta$ CD is bound in an orientation in which its interior is exposed to solvent, rather than (for example) being occupied by an amino acid side chain. The residual current observed in the presence of a guest may represent ions flowing between the outer surface of the cyclodextrin ring and the  $\alpha$ HL wall (Gu et al., 1999). Finally, the idea of a discrete binding site for  $\beta$ CD within the lumen of the  $\alpha$ HL pore is strengthened by the existence of mutants with enhanced affinity for  $\beta$ CD and other cyclodextrins (Gu et al., 1999, 2000). For example, in the case of M113N, the  $K_d^{app}$  is decreased from  $3.6 \times 10^{-3}$  M to  $1.5 \times 10^{-7}$  M at pH 7.5,  $-40$  mV. Thus, the situation with cyclodextrin adapters differs from that with flexible polymers such as PEG or polynucleotides, which sustain brief encounters with the lumen or rapidly pass through it without lodging at a defined site (Kasianowicz et al., 1996; Bezrukov, 2000).

### The binding site for $\beta$ CD can be accessed from the *trans* but not the *cis* side of the bilayer

$\beta$ CD can reach its binding site in the lumen of the  $\alpha$ HL pore from the *trans* side of the membrane (Fig. 2, C–E), but it has no effect when applied from the *cis* side (Fig. 2 B), even at extremes of pH and transmembrane potential. The *cis* entrance to the lumen is wider than the *trans* entrance (Fig. 1), so binding from the *cis* side must be hindered by an internal barrier (Merzlyak et al., 1999), which we suggest is formed by the rings of Glu-111 and Lys-147 side chains (Song et

al., 1996). Interestingly, *cis* binding events of  $\beta$ CD can be detected with the mutant E111N/M113N/K147N, in which the internal barrier is removed, and the dwell times ( $\tau_{off}$ ) are very similar whether  $\beta$ CD binds from the *trans* or the *cis* entrance, again suggesting a single site (L.-Q. Gu and S. Cheley, unpublished observations).

### Voltage- and pH-dependence of the interaction of $\beta$ CD with the $\alpha$ HL pore: ruling out familiar mechanisms

#### Woodhull's mechanism for a charged blocker

The affinity of a charged blocker for a site within the lumen of a channel is voltage-dependent and described by the equation of Woodhull (Woodhull, 1973; Hille, 1991):

$$K_d(V) = K_d(0)\exp(-z_b F \delta \Delta V / RT) \quad (2)$$

when a blocker of charge  $z_b$  is applied from the *trans* side of the bilayer, and  $\delta$  is the distance from the *trans* side to the position at which the blocker binds.  $\delta \sim 0.5$  for  $\beta$ CD (Fig. 1 A and Gu et al., 1999).

The only potentially ionizable groups on  $\beta$ CD are the 21 hydroxyls, but two strong arguments can be made against a charged form of  $\beta$ CD binding with the lumen of  $\alpha$ HL. First, the  $pK_a$  value of an unperturbed aliphatic hydroxyl group is high,  $pK_a \approx 16$ . Although the  $pK_a$  value is shifted to  $pK_a = 12.2$  in  $\beta$ CD, by statistical and environmental effects (Szejtli, 1998), the signs of the observed effects of pH and voltage on binding are the opposite to what are predicted from Eq. 2. For example,  $\beta$ CD binds weakly at high pH and negative potentials, when it would be negatively charged

and driven into the channel by the electrical potential. The dipole moment of βCD has been calculated to be about 3 D in a conformation close to that determined by x-ray crystallography (Botsi et al., 1996). Therefore, the free energy of transfer of a neutral but oriented βCD molecule into the transmembrane field would be expected to make only a minor contribution to the free energy of binding of βCD to αHL (Moczydlowski, 1986).

#### Voltage-dependent two-state conformational change of the protein

A second possibility is that there are two states of the αHL pore that exist in a voltage-dependent equilibrium.

$$p_b/p_a = \exp(-\Delta G(0) + z_p F \delta \Delta V / RT) \quad (3)$$

where “b” is the state of αHL that binds βCD, while “a” does not; and  $z_p$  is a charge on the protein that moves a distance  $\delta$  away from the *trans* side of the membrane when state “a” is converted to state “b.”

This model would accommodate, at least qualitatively, the observed  $K_d^{app}$  values ( $K_d^{app} = K_d \cdot (1 + \exp((\Delta G(0) - z_p F \delta \Delta V) / RT))$ ), assuming that at least two residues carry the charge  $z_p$ , so that the mobile charge can switch from positive to negative with pH. For example, at low pH, a positively charged group might be pushed toward the *trans* side in a negative transmembrane potential poisoning the equilibrium in favor of state “b,” thereby decreasing  $K_d^{app}$ . By contrast, at high pH the first ionizable group would be titrated to a neutral value, allowing a second negatively charged group to be pushed away from the *trans* side in the negative potential, poisoning the equilibrium in favor of state “a,” thereby increasing  $K_d^{app}$ . The proposed mechanism would account for the variation of  $K_d^{app}$  with voltage and pH, but there is a major difficulty with the model in that the  $k_{off}$  value for state “b,” the dissociation rate constant of βCD

from its binding site, should not vary with pH and voltage, as it so clearly does (Fig. 5, *A* and *B*).

#### A viable model for the voltage- and pH-dependence of the interaction of βCD with the αHL pore

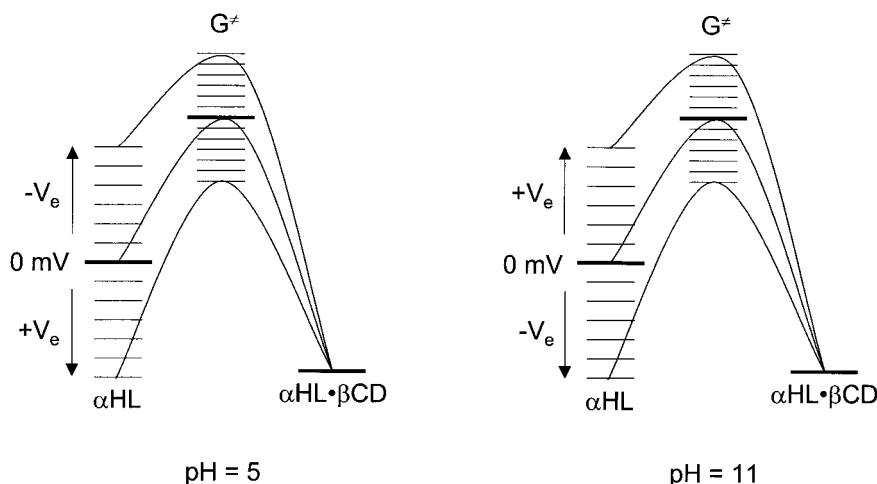
A third model involves a continuous change in the free energy of αHL or αHL · βCD (or both) as a function of the membrane potential. For example, βCD might bind to αHL in a single step by induced fit (Koshland et al., 1966), rather than through one of two states required by the second model. In a *simplified version* of the third model, the free energy of αHL · βCD remains unaltered in an applied field, while the free energy of αHL varies as  $\Delta G = -z_p F \delta \Delta V$  (Fig. 6). The dependence of  $K_d$  on voltage is then given by a relation with the same form as Eq. 3:

$$K_d(V) = K_d(0) \exp(+z_p F \delta \Delta V / RT) \quad (4)$$

Despite the similarity between Eqs. 3 and 4, it is clear that the free energy barrier to the transition state ( $\Delta G^\ddagger$ ) varies in model 3 (Fig. 6), with a dependence on voltage that would account qualitatively for the variation in  $k_{on}$  and  $k_{off}$  (Fig. 5). The use of  $z_p$  and  $\delta$  imply that a localized charge moves as βCD binds. The same result would obtain if, when βCD binds, there were a change in the dipole moment of the protein with contributions from several regions of the molecule (Moczydlowski, 1986).

At pH 5.0 and pH 11.0, and at low potentials, plots of  $\log K_d^{app}$  versus  $\Delta V$  (Fig. 5 *C*) can be fitted to straight lines as predicted by Eq. 4, yielding  $z_p \delta$  values of +0.60 and −0.61, respectively. These data imply that at low pH, positive charge on the protein moves toward the *trans* side of the bilayer as βCD binds; hence, binding is favored at negative potentials. By contrast, at high pH, negative charge must move toward the *trans* side when βCD binds. At interme-

FIGURE 6 The pH- and voltage-dependent interaction of βCD with αHL depicted as conceptual free energy profiles. In this *simplified* rendition, the occupied form of the protein, αHL · βCD, is supposed to be unaffected by voltage. The free energy of the unoccupied form, αHL, is voltage-dependent. For example, at low pH a positive charge on the pore might be located part way through the lipid bilayer in the unoccupied form of the protein. Thus, a negative potential would increase the free energy of the unoccupied protein relative to the occupied form and the binding of βCD would be favored.



diate pH values and at extremes of pH, plots of  $\log K_d^{\text{app}}$  versus  $\Delta V$  are not linear and a more complex model would be required to fit the data, which is not warranted given our present knowledge of the system.

The third model implies that the conformational change of  $\alpha\text{HL}$  that occurs when  $\beta\text{CD}$  binds (Fig. 6) does not occur in the absence of  $\beta\text{CD}$ , i.e., that the conformationally altered state of the protein is separated by an insurmountable free energy barrier in the absence of  $\beta\text{CD}$ . Alternatively, the conformationally altered, but unoccupied, state and intermediate conformational states might be energetically accessible, in which case the structure of the protein would gradually change with membrane potential to forms with increased or decreased affinity for  $\beta\text{CD}$ . This effect of voltage would also satisfy Eq. 4 and the experimental observations on  $k_{\text{off}}$ . Model 2 is an extreme version of this last case in which there is not a gradual change in structure, but two states separated by a surmountable barrier.

### pH-dependence of the properties of the $\alpha\text{HL}$ pore

Several properties of the  $\alpha$ -hemolysin pore are pH-dependent, including the unitary conductance, ion selectivity, and magnitude of single-channel noise (Menestrina, 1986; Bezrukov and Kasianowicz, 1993; Kasianowicz and Bezrukov, 1995; Krasilnikov et al., 1997). Most relevant to the present work is the finding that the interactions of neutral PEG molecules with the lumen of the transmembrane channel vary with pH; at lower pH values, the size of polymers that interact with the lumen is reduced (Bezrukov and Kasianowicz, 1997). There is not enough in common between these experiments and the present work to determine whether the same ionizable groups on the protein are involved in both cases. For example, the interactions of PEG with the channel lumen are weak compared with those of the cyclodextrins. Nevertheless, it is interesting that in both cases the kinetics of binding of a neutral molecule are affected.

### CONCLUSIONS

We have measured the interaction of the adapter molecule  $\beta\text{CD}$  with WT- $\alpha\text{HL}$  over a wide range of pH values and transmembrane potentials. When extrapolated to a transmembrane potential of 0 mV, the  $K_d^{\text{app}}$  values for  $\beta\text{CD}$  show little variation over the range pH = 5.0–11.0. While this suggests that ionizable groups play no role in the interaction of  $\alpha\text{HL}$  with  $\beta\text{CD}$  at 0 mV, the situation is in fact more complex, because compensating changes in  $k_{\text{on}}^{\text{app}}$  and  $k_{\text{off}}$  occur.  $K_d^{\text{app}}$  values for  $\beta\text{CD}$  vary continuously with voltage. Because  $\beta\text{CD}$  is a neutral molecule, this finding suggests that charge movement on the protein is associated with the binding event. Because  $k_{\text{off}}$  the dissociation rate constant of  $\beta\text{CD}$  from its binding site, also varies continuously with

voltage, a simple two-state model, in which there are high- and low-affinity forms of  $\alpha\text{HL}$ , is ruled out. Instead, a model is suggested that features a single unoccupied state of the channel with a free energy relative to  $\alpha\text{HL} \cdot \beta\text{CD}$  that is voltage-dependent. For applications in sensors, it is important that the dwell time of an adapter within the  $\alpha\text{HL}$  pore be as prolonged as possible. The data presented here show that the dwell time can be manipulated with pH and voltage. These tactics might be combined with increases in dwell time obtained by mutagenesis (L.-Q. Gu and S. Cheley, unpublished data) to improve the characteristics of  $\alpha\text{HL}$  pores as sensor elements.

We thank Stephen Cheley for samples of  $\alpha$ -hemolysin, Sean Conlan for help with the figures, and Stephen Cheley and Orit Braha for their advice.

This work was supported by DOE, ONR, and DARPA.

### REFERENCES

- Al-yahyaee, S. A. S., and D. J. Ellar. 1996. Cell targeting of a pore-forming toxin, CytA  $\delta$ -endotoxin from *Bacillus thuringiensis* subspecies *israelensis*, by conjugating CytA with anti-Thy1 monoclonal antibodies and insulin. *Bioconjugate Chem.* 7:451–460.
- Bayley, H. 1997. Building a door into cells. *Sci. Am.* 277:62–67.
- Bayley, H. 1999. Designed membrane channels and pores. *Curr. Opin. Biotechnol.* 10:94–103.
- Bayley, H., O. Braha, and L.-Q. Gu. 2000. Stochastic sensing with protein pores. *Adv. Mater.* 12:139–142.
- Bezrukov, S. M. 2000. Ion channels as molecular Coulter counters to probe metabolite transport. *J. Membr. Biol.* 174:1–13.
- Bezrukov, S. M., and J. J. Kasianowicz. 1993. Current noise reveals protonation kinetics and number of ionizable sites in an open protein ion channel. *Phys. Rev. Lett.* 70:2352–2355.
- Bezrukov, S. M., and J. J. Kasianowicz. 1997. The charge state of an ion channel controls neutral polymer entry into its pore. *Eur. Biophys. J.* 26:471–476.
- Bhakdi, S., R. Füssle, and J. Trantum-Jensen. 1981. Staphylococcal  $\alpha$ -toxin: oligomerization of hydrophilic monomers to form amphiphilic hexamers induced through contact with deoxycholate micelles. *Proc. Natl. Acad. Sci. U.S.A.* 78:5475–5479.
- Botsi, A., K. Yannakopoulou, E. Hadjoudis, and J. Waite. 1996. AM1 calculations on inclusion complexes of cyclomaltoheptaose ( $\beta$ -cyclodextrin) with 1,7-dioxaspiro[5.5]undecane and nonanal, and comparison with experimental results. *Carbohydrate Res.* 283:1–16.
- Braha, O., B. Walker, S. Cheley, J. J. Kasianowicz, L. Song, J. E. Gouaux, and H. Bayley. 1997. Designed protein pores as components for biosensors. *Chem. Biol.* 4:497–505.
- Chang, C.-Y., B. Niblack, B. Walker, and H. Bayley. 1995. A photogenerated pore-forming protein. *Chem. Biol.* 2:391–400.
- Corradini, R., A. Dossena, R. Marchelli, A. Panagia, G. Sartor, M. Saviano, A. Lombardi, and V. Pavone. 1996. A modified cyclodextrin with a fully encapsulated dansyl group: self inclusion in the solid state and in solution. *Chem. Eur. J.* 2:373–381.
- D'Souza, V. T., and K. B. Lipkowitz. 1998. Cyclodextrins. *Chem. Rev.* 98:1741–2076.
- Eroglu, A., M. J. Russo, R. Bieganski, A. Fowler, S. Cheley, H. Bayley, and M. Toner. 2000. Intracellular trehalose improves the survival of cryopreserved mammalian cells. *Nat. Biotechnol.* 18:163–167.
- Füssle, R., S. Bhakdi, A. Sziegoleit, J. Trantum-Jensen, T. Kranz, and H.-J. Wellensiek. 1981. On the mechanism of membrane damage by *Staphylococcus aureus*  $\alpha$ -toxin. *J. Cell Biol.* 91:83–94.



- Gouaux, E. 1998.  $\alpha$ -Hemolysin from *Staphylococcus aureus*: an archetype of  $\beta$ -barrel, channel-forming toxins. *J. Struct. Biol.* 121:110–122.
- Gu, L.-Q., O. Braha, S. Conlan, S. Cheley, and H. Bayley. 1999. Stochastic sensing of organic analytes by a pore-forming protein containing a molecular adapter. *Nature*. 398:686–690.
- Gu, L.-Q., M. Dalla Serra, J. B. Vincent, G. Vigh, S. Cheley, O. Braha, and H. Bayley. 2000. Reversal of charge selectivity in transmembrane protein pores by using noncovalent molecular adapters. *Proc. Natl. Acad. Sci. U.S.A.* 97:3959–3964.
- Hanke, W., and W.-R. Schlue. 1993. Planar lipid bilayers. Academic Press, London.
- Hille, B. 1991. Ionic channels of excitable membranes. Sinauer, Sunderland, MA.
- Howorka, S., L. Movileanu, X. Lu, M. Magnon, S. Cheley, O. Braha, and H. Bayley. 2000. A protein pore with a single polymer chain tethered within the lumen. *J. Am. Chem. Soc.* 122:2411–2416.
- Kasianowicz, J. J., and S. M. Bezrukov. 1995. Protonation dynamics of the  $\alpha$ -toxin channel from spectral analysis of pH-dependent current fluctuations. *Biophys. J.* 69:94–105.
- Kasianowicz, J. J., E. Brandin, D. Branton, and D. W. Deamer. 1996. Characterization of individual polynucleotide molecules using a membrane channel. *Proc. Natl. Acad. Sci. U.S.A.* 93:13770–13773.
- Korchev, Y. E., G. M. Alder, A. Bakhranov, C. L. Bashford, B. S. Joomun, E. V. Sviderskaya, P. N. R. Usherwood, and C. A. Pasternak. 1995. *Staphylococcus aureus*  $\alpha$ -toxin-induced pores: channel-like behavior in lipid bilayers and patch clamped cells. *J. Membr. Biol.* 143:143–151.
- Koshland, D. E., G. Neméthy, and D. Filmer. 1966. Comparison of experimental binding data and theoretical models in proteins. *Biochemistry*. 5:365–385.
- Krasilnikov, O. V., M.-F. P. Capistrano, L. N. Yuldasheva, and R. A. Nogueira. 1997. Influence of Cys-130 *S. aureus*  $\alpha$ -toxin on planar lipid bilayer and erythrocyte membranes. *J. Membr. Biol.* 156:157–172.
- Menestrina, G. 1986. Ionic channels formed by *Staphylococcus aureus*  $\alpha$ -toxin: voltage-dependent inhibition by divalent and trivalent cations. *J. Membr. Biol.* 90:177–190.
- Merzlyak, P. G., L. N. Yuldasheva, C. G. Rodrigues, C. M. M. Carneiro, O. V. Krasilnikov, and S. M. Bezrukhov. 1999. Polymeric nonelectrolytes to probe pore geometry: application to the  $\alpha$ -toxin transmembrane channel. *Biophys. J.* 77:3023–3033.
- Moczydlowski, E. 1986. Single-channel enzymology. In *Ion Channel Reconstitution*. C. Miller, editor. Plenum Press, New York. 75–113.
- Montal, M., and P. Mueller. 1972. Formation of bimolecular membranes from lipid monolayers and study of their electrical properties. *Proc. Natl. Acad. Sci. U.S.A.* 69:3561–3566.
- Panchal, R. G., E. Cusack, S. Cheley, and H. Bayley. 1996. Tumor protease-activated, pore-forming toxins from a combinatorial library. *Nat. Biotechnol.* 14:852–856.
- Pederzoli, C., G. Belmonte, M. D. Serra, P. Macek, and G. Menestrina. 1995. Biochemical and cytotoxic properties of conjugates of transferrin with equinatoxin II, a cytolytic toxin from a sea anemone. *Bioconjugate Chem.* 6:166–173.
- Saenger, W., J. Jacob, K. Gessler, T. Steiner, D. Hoffman, H. Sanbe, K. Koizumi, S. M. Smith, and T. Takaha. 1998. Structures of the common cyclodextrins and their larger analogues—beyond the doughnut. *Chem. Rev.* 98:1787–1802.
- Schneider, H.-J., F. Hackett, V. Rüdiger, and H. Ikeda. 1998. NMR studies of cyclodextrins and cyclodextrin complexes. *Chem. Rev.* 98:1755–1785.
- Song, L., M. R. Hobaugh, C. Shustak, S. Cheley, H. Bayley, and J. E. Gouaux. 1996. Structure of staphylococcal  $\alpha$ -hemolysin, a heptameric transmembrane pore. *Science*. 274:1859–1865.
- Szejtli, J. 1998. Introduction and general overview of cyclodextrin chemistry. *Chem. Rev.* 98:1743–1753.
- Walker, B., O. Braha, S. Cheley, and H. Bayley. 1995. An intermediate in the assembly of a pore-forming protein trapped with a genetically-engineered switch. *Chem. Biol.* 2:99–105.
- Walker, B. J., M. Krishnasastri, L. Zorn, J. J. Kasianowicz, and H. Bayley. 1992. Functional expression of the  $\alpha$ -hemolysin of *Staphylococcus aureus* in intact *Escherichia coli* and in cell lysates. *J. Biol. Chem.* 267:10902–10909.
- Woodhull, A. M. 1973. Ionic blockage of sodium channels in nerve. *J. Gen. Physiol.* 61:687–708.
- Ziegler, C., and W. Göpel. 1998. Biosensor development. *Curr. Opin. Chem. Biol.* 2:585–591.